NANO REVIEW

Directed Self-Assembly: Expectations and Achievements

Prashant Kumar

Abstract Nanotechnology has been a revolutionary thrust in recent years of development of science and technology for its broad appeal for employing a novel idea for relevant technological applications in particular and for mass-scale production and marketing as common man commodity in general. An interesting aspect of this emergent technology is that it involves scientific research community and relevant industries alike. Top–down and bottom–up approaches are two broad division of production of nanoscale materials in general. However, both the approaches have their own limits as far as large-scale production and cost involved are concerned. Therefore, novel new techniques are desired to be developed to optimize production and cost. Directed self-assembly seems to be a promising technique in this regard; which can work as a bridge between the top–down and bottom–up approaches. This article reviews how directed self-assembly as a technique has grown up and outlines its future prospects.

Keywords Nanotechnology · Directed self-assembly · Template assisted growth · Field-induced growth

Introduction

Nanotechnology promises to revolutionize the way we think about, but more importantly create new materials. The key to making this promise a reality is a commitment to fundamental research in critical areas including synthesis, fabrication, and characterization of nanoscale

P. Kumar (✉)
Jawaharlal Nehru Centre for Advanced Scientific Research,
Bangalore 560064, India
e-mail: prashantkumar@jncasr.ac.in

components. Nanoparticles have attracted wide attention as such components due to their unique size-dependent properties including, superparamagnetism, chemilumiescence, and catalysis. To fully harness the potential capabilities of nanoparticles, we need to develop new methods to assemble them into useful patterns or structures. These self-assembled structures promise new opportunities for developing miniaturized optical, electronic, optoelectronic, and magnetic devices.

As the size of device features becomes increasingly smaller, conventional lithographic processes are limited. Alternative routes need to be developed to circumvent this difficulty. As conventional fabrication technologies, such as optical lithography, develop, they begin to run up against fundamental limits. New measurement methods are needed to understand and help mitigate the effects of those limits. In addition, novel fabrication techniques are required to help extend both the lifetime and range of application of existing techniques. Directed self-assembly is an emergent technology of current interest [1–10]. Directed self-assembly approach is still going through developmental phases, and leverages existing patterning methods by combining them with self-organizing systems, to create manufacturing techniques that can be readily integrated into existing processes. Directed self-assembly technique can be appropriately employed to yield functional nanostructures e.g. nanowires and organized array of nanodots.

As the size scale of device features becomes increasingly smaller, conventional lithographic processes are limited. Alternative routes need to be developed to circumvent this hard stop. As conventional fabrication technologies, such as optical lithography, develop, they begin to run up against fundamental limits. New measurement methods are needed to understand and help mitigate the

effects of those limits. In addition, novel fabrication techniques are required to help extend both the lifetime and range of application of existing techniques. Directed self-assembly is one of the emergent technologies which find interest to the researchers currently [1–10]. Directed self-assembly approach is still going through developmental phases and leverages existing patterning methods by combining those with self-organizing systems to create manufacturing techniques that can be readily integrated into existing processes. Directed self-assembly technique can be appropriately employed to yield functional nanostructures e.g. nanowires and arrays of organized nanodots.

Spontaneous self-assembly is introduced as an evaporation-induced phenomenon that yields random patterns. Among guided self-assembly approaches (employing some guiding agent to nanoparticles or vapour of atoms), template-guided and field-guided assemblies are two approaches. For template-guided assembly, existing surface atomic pattern or nano/micro features as templates are made use of. Among field guided assembly, use of pressure gradient, magnetic field, electric field, electron beam, light and laser, etc. are few to count with. The present article reviews the progress so far in the direction of establishment of directed self-assembly as a reproducible and robust technique and its future prospects for its usage at industrial scale.

Spontaneous Self-Assembly

The use of spontaneous self-assembly as a lithography- and external field-free which means to construct well-ordered often intriguing structures has received much attention for its ease of organizing materials on the nanoscale into ordered structures and producing complex, large-scale structures with small feature sizes. An extremely simple route to intriguing structures is the evaporation-induced self-assembly (EISA) [11–18] of polymers and nanoparticles from a droplet on a solid substrate. However, flow instabilities within the evaporating droplet often result in non-equilibrium and irregular dissipative structures, e.g., randomly organized convection patterns and stochastically distributed multi-rings. [11–14, 16, 19–22]. Therefore, fully utilizing evaporation as a simple tool for creating well-ordered structures with numerous technological applications requires precise control over several factors, including evaporative flux, solution concentration, and the interfacial interaction between solute and substrate [23–31] (Fig. 1).

As shown in Fig. 1a, there is no apparent visible spatial orderliness of nanoparticles in the nickel thin film of thickness 50 nm coated onto borosilicate glass substrate in the process of resistive thermal evaporation. The metal particle size and size distribution depends on the deposition

conditions, e.g., electrical power used for thermal evaporation (which determines remaining energy of the adatoms when it lands onto the substrate), wettability offered by the substrate to the thin film material (substrate and thin film material), diffusivity of thin film material atoms on the substrate (substrate temperature) etc.

After transport the substrates and conditions on the substrate surface play an important role in determining the microstructural evolution of the films. It is pertinent at this point to recall the process of condensation of vapor into thin films on substrates [32]. Initially small nuclei, depending on the effective surface energy available, form on the substrate. These satisfy the condition of nucleation (supersaturation ratio > 1), which in turn is dependent on the substrate material itself. Once a few nuclei form, they work as nucleation centers. Coalescence between nuclei occurs, and this finally gives rise to the growth of continuous layers. Nanoparticulate formation in particular can be attributed to the metal–substrate interactions. Energetics decides the contact angle of the condensate onto the substrate, residual strain, and size and shape of the nanoparticles deposited. The capillary model predicts that free energy of formation of condensed aggregate goes through a maximum [32]. With heating of the substrate, densification occurs, and the grain wall boundary width is thinned. At RT deposition conditions, because sufficient energy is not available for mobility of adatoms on the substrate surface, the size is not enhanced much due to coalescence.

Occasionally, some short distance orderlinesses (as shown in Fig. 1b for nickel thin film growth on [311] silicon substrate by resistive thermal evaporation at room temperature) have been observed in thin films achieved by thermal evaporation; whose origin can be traced in the atomic scale linear edges formed while cutting the substrate in particular plane which virtually works as template for few layers of thin film growth.

The organization of inorganic nanostructures within self-assembled organic or biological templates [33–43] is receiving the attention of scientists interested in developing functional hybrid materials. Previous efforts have concentrated on using such scaffolds [39, 44] to spatially arrange nanoscopic elements as a strategy for tailoring the electrical, magnetic, or photonic properties [40–43, 45–48] of the material. Recent theoretical arguments [48–50] have suggested that synergistic interactions between self-organizing particles and a self-assembling matrix material can lead to hierarchically ordered structures. Lin et al. [51] has recently demonstrated (as shown in Fig. 2) self-directed self-assembly of ferritin-PEG nanoparticles on P2VP-b-PEO copolymer thin film.

MWNT has been aligned [31] (as shown in Fig. 3b, c) on evaporation-induced self-assembly of MEH-PPV rings in a sphere-on-flat geometry (as shown in Fig. 3a).

Fig. 1 AFM image of 50 nm Ni thin film grown on **a** BSG and **b** Silicon substrates (Author's unpublished work)
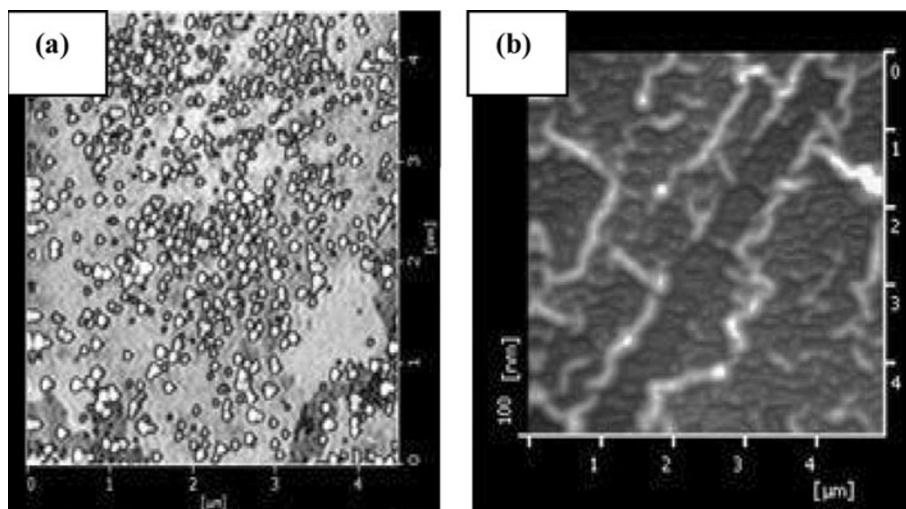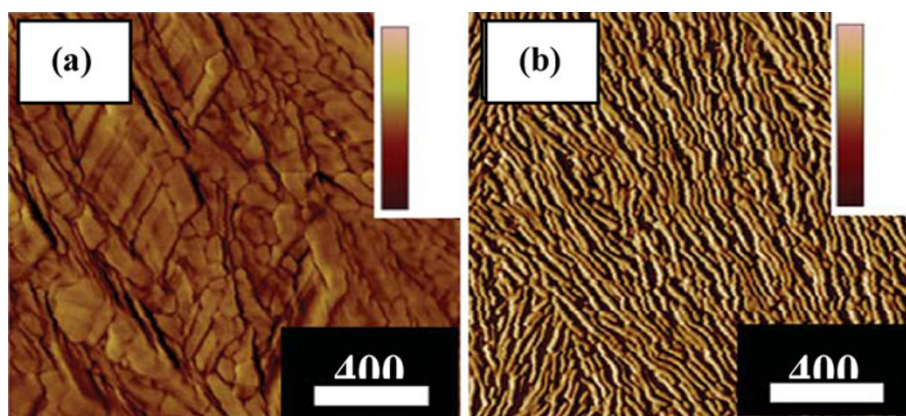

Fig. 2 Structure of a P2VP-b-PEO thin film after annealing for **a** without ferritin-PEG nanoparticles and **b** with ferritin-PEG nanoparticles [51]

Guided Self-Assembly

The assembly of nanoparticles into ordered architectures is a potential route to achieve further construction and miniaturization of electronic and optical devices. Among guided self-assemblies, (a) template-guided self-assemblies and (b) field-guided self-assemblies are two broad divisions.

Template-Guided Self-Assembly

Among template-guided self-assemblies, use of physical templates, chemical templates and biological templates are three ways to achieve orientation in the growth features. Physical template has to do with physical existence of ridge, depth, patterning on the substrate surface. Physical templates can be an atomic pattern or ridges, nano/microscale pre-existing pattern on the substrate in the form of pores or linear features or two-dimensional architectures. Unsatisfied bonds can in principle work as chemical templates. Use of DNA as a biological template for guided self-assembly has been attracting attention to biochemists and biophysicists.

Physical Template

Advantages with physical template-assisted fabrication of nanowires lie in the fact that they combine fabrication with organization and solve integration issues (eliminating the need to manipulate individual nanowires). Issues related to contacts for electrical and magnetotransport are also solved. Moreover, physical vapour deposition techniques such as evaporation, sputtering and Pulsed Laser Deposition (PLD) are well-known industrially applicable techniques, and hence fabrication of nanowires using these approaches is also expected to be very useful.

Use of physical templates gives rise to the growth of nanomaterials at pre-defined position eliminating the need of post-growth manipulation and providing the ease of electrical connections for further characterizations. Porous anodic alumina [53–56] and silica [57] membrane have been widely used to grow patterned nanodot arrays in a routine manner by scientific community. Recently, Ru nanostructure fabrication has been reported [58], using an anodic aluminium oxide nanotemplate and highly conformal Ru atomic layer deposition (as shown in Fig. 4).
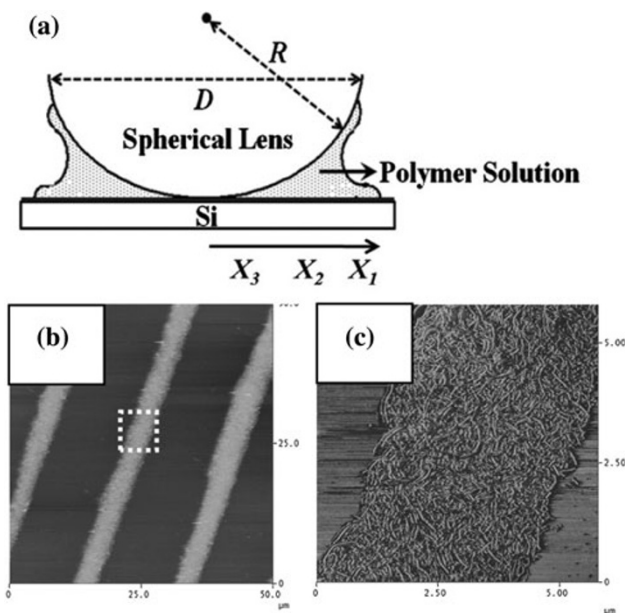
Fig. 3 a Evaporation-induced ring formation technique for sphere-on-flat geometry, **b** AFM height image of highly ordered MWNT rings at the region in between ×1 and ×2 as shown in Fig. 3a. **c** The close-up AFM topographical images marked in b. The image size is $50 \times 50 \ \mu m^2$ in b, and $5.8 \times 5.8 \ \mu m^2$ in c. The z scale is 50 nm for all images [52]

Fig. 4 Ru nanowire array device on Ti/Si substrate: **a** the tilt view FE-SEM image, **b** I–V characteristics showing ohmic contact between the end of the Ru nanowires and the Ti bottom electrode [58]

Such templates give rise to the growth of nanodots, vertical nanowires, which can be controllably used to fabricate FET devices, magnetic tunnel junction devices and devices for optical applications. Fabrication of nanomaterials using porous alumina templates has been reviewed [59]. However, use of in-plane growth of nanowires and array of nanodots seems to be more promising. Ravi Shankar et al. [60] used linear grooves appearing on m-plane alumina after the heating at 1,800°C for long hours as a template for CVD growth to achieve linear in-plane growth features in the form of nanowires and array of nanodots (as shown in Fig. 5a). They reported that the growth in most of the cases occurs at the top ridge of the groove which they attributed to electric field singularity positions.

$$E = k(\rho)^{-\beta} \text{ where } \beta = (\pi - \alpha)/(2\pi - \alpha)$$

where k is a constant, and α is the angle of the wedge.

Brown et al. [61] have achieved nanowires inside the lithographically fabricated trenches using nanocluster source. The nanoclustered nanowires usually grow at the apex of the trench (as shown in Fig. 5b).

If the V-groove trench be shallow, then more vapour would get access inside the trench, and therefore, one can expect nanowire growth on the trench sidewalls inside. Current author has exploited this aspect of thin film growth inside the V-groove trench template to achieve nanowire
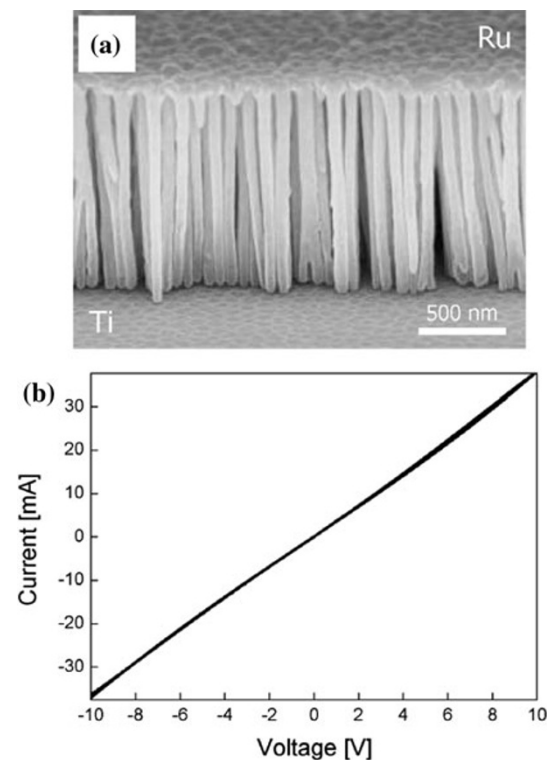
growth on the apex and sidewalls of the trenches. They have demonstrated that very long nanowires can be fabricated with good control of diameter [62–64]. Diameter/depth (D/H) ratio determines whether any kind of linear self-assembly (nanowire or array of nanodots) would occur or not. For large D/H ratio, shadowing would not be sufficient to give rise to any guided growth, in such a case, usual isotropic thin film growth occurs. Nanowire diameter is the deposition thickness-dependent. Thin film material–substrate combination is also crucial for providing perfect dewetting conditions (as shown in Fig. 6). This figure demonstrates the growth features of nickel by thermal evaporation (SEM image in Fig. 6a) and AFM image in Fig. 6b), nickel by pulsed laser deposition (Fig. 6c), gold (Fig. 6d), silicon (Fig. 6e) and indium (Fig. 6f) nanowires. In all the cases, first array of nanodots grows, and then at larger deposition thickness of the material, nanowire growth takes place. There is a window of D/H ratio, which is favourable for nanowire growth features.

Chemical Template

Gold-tipped CdSe rods (nanodumbbells) were solubilized in an aqueous phase and self-assembled in a head-to-tail manner using biotin disulphide and avidin [65]. The disulphide

Fig. 5 a Growth of array of nanobeads on the edges formed on m-plane alumina surface after heating at 1,800°C [39]. **b** Nanocluster nanowire growth inside the lithographically drawn trenches [61]
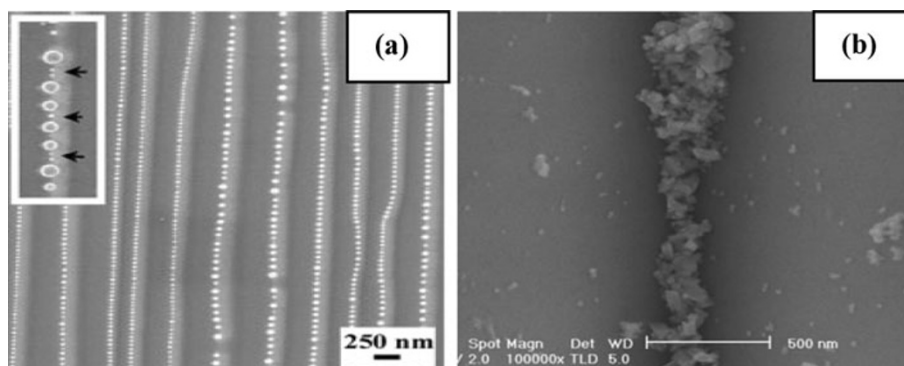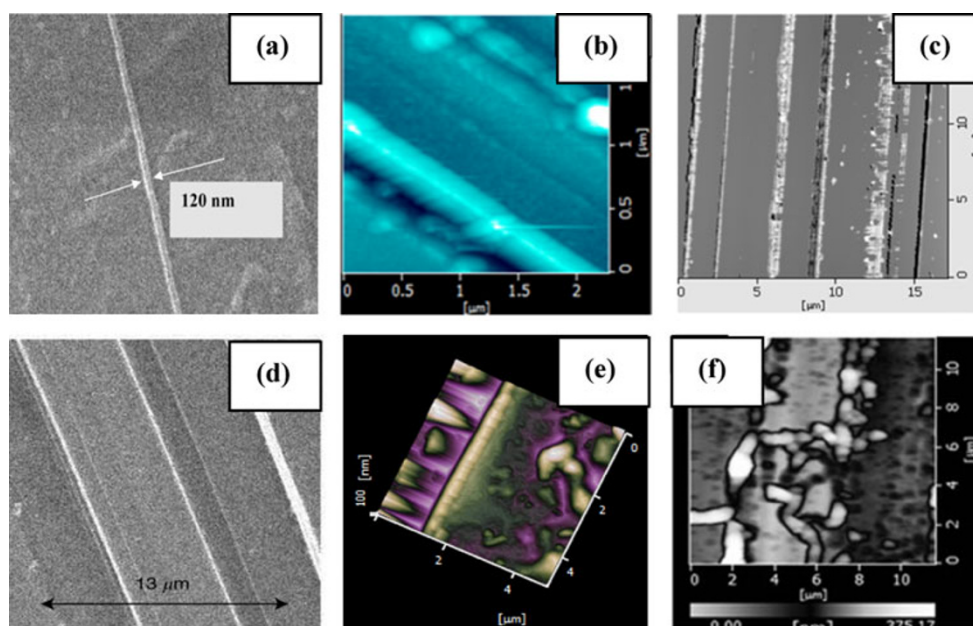

Fig. 6 a SEM image for nickel nanowire growth for 50 nm thin film coating, **b** AFM image for the Ni nanowire growth, **c** AFM image of Ni nanowire grown in PLD, **d** SEM image of gold nanowire, **e** AFM image of Si nanowire, **f** AFM image of In nanowire [62, 63]

end of the biotin molecule attaches to the gold tip of the nanodumbbell, and the biotin end of the molecule is able to conjugate to an avidin protein. The avidin can strongly conjugate up to four biotin molecules. Changing the ratios of biotin to nanodumbbells leads to the formation of dimers, trimers, and flowerlike structures. To further improve the distribution of chain lengths, a separation method based upon weight was applied using a concentration gradient. The gold tips provide effective anchor points for constructing complex nanorod structures by self-assembly. Metal-directed self-assembly of two- and three-dimensional synthetic receptors has been reviewed recently [66].

Biological Template

Biomolecule-directed strategies have shown great promise in assembling nanoparticles into a wide diversity of architectures, because of their high efficiency, high specificity and genetic programmability [67]. Such nanoassembled materials have been shown to have potential applications in new detection systems, such as biosensors [68] and chemical sensors [69, 70], and in the construction of nanoelectronic devices [71]. DNA-directed self-assembly of gold nanoparticles into binary and ternary Nanostructures has recently been demonstrated [72] as shown in Fig. 7, where S_1 ends with –SH and S_2 ends with –HS. Two sizes of gold nanoparticles (10 and 30 nm average diameters) were used for the purpose.

Field Guided Self-Assembly

Among field-guided self-assemblies, use of pressure gradient, electric field, magnetic field, light, laser, etc. are some to count with.

Flow-Induced Self-Assembly

Ordering induced by shear flow can be used [73] to direct the assembly of particles in suspensions. Flow-induced ordering is determined by the balance between a range of
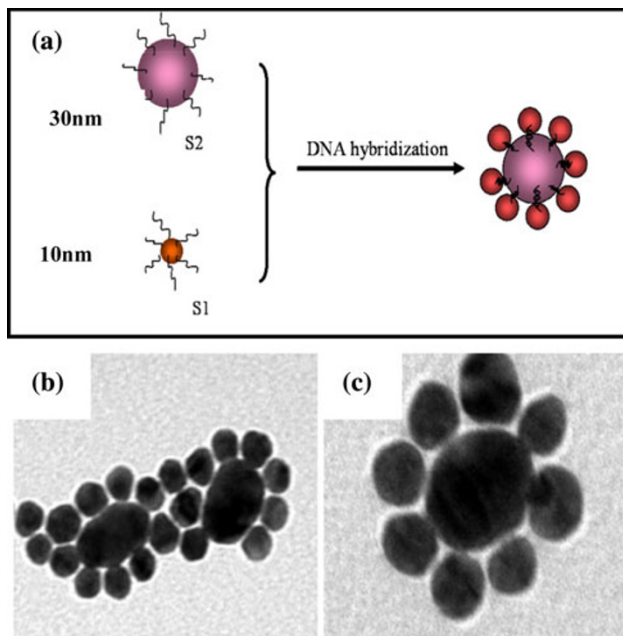
Fig. 7 **a** Illustration of the strategy to prepare 'satellite'-shaped assemblies. **b**, **c** A nanoparticle satellite structure obtained from the reaction involving 9:1 S_1-modified 10 nm particles/S_2-modified 30 nm particle [72]
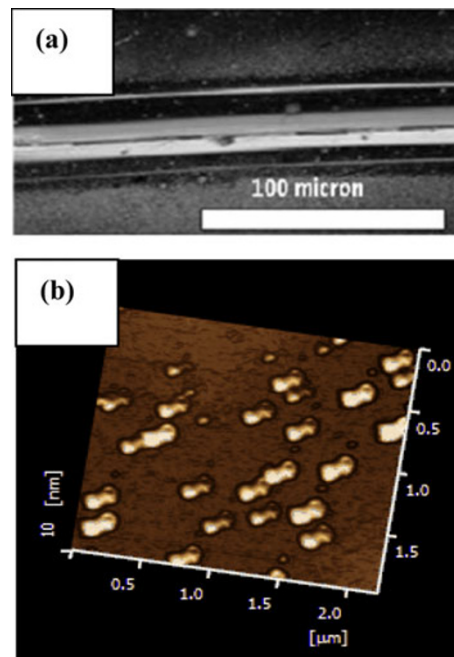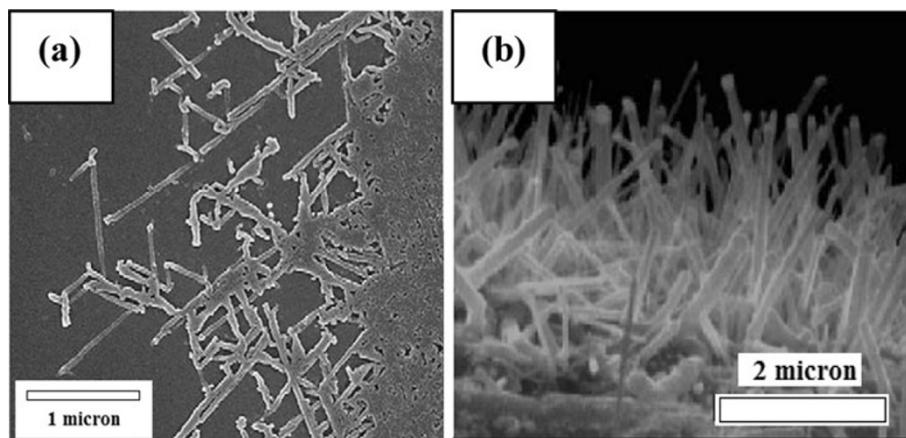

Fig. 9 **a** SEM image of electric field–induced growth of microwide trenches. **b** AFM image of silicon nanocrystals grown on silicon surface by electric field–induced nanostructuring technique [78]

forces, such as direct interparticle, Brownian, and hydrodynamic forces. The latter are modified when dealing with viscoelastic rather than Newtonian matrices. In particular, 1D stringlike structures of spherical particles have been observed to form along the flow direction in shear thinning viscoelastic fluids, a phenomenon not observed in Newtonian fluids at similar particle volume fractions. Here, we report on the formation of freestanding crystalline patches in planes parallel to the shearing surfaces.

Electric Field–Induced Assembly

There are few reports on electric field–induced ordering and assembly [7, 10]. Electrostatic self-assembly of

polystyrene microspheres by using chemically directed contact electrification has been reported [74]. Directed self-assembly of quantum dots in a nematic liquid crystal [75] has also been reported earlier. Field-added lateral MIC of silicon has been reported to give rise to aligned nanostructures [76]. Electric field–induced growth of vertical indium oxide nanowires also has been reported [77] (Fig. 8).

Current author has employed electric field for nanostructuring various metallic and semiconducting thin films and semiconductor bulk surfaces. Electric field applied to silicon bulk surfaces [78] gives rise to field evaporation in the direction of electric field and trenches form in that direction (as shown in Fig. 9a). The material evaporated

Fig. 8 **a** Field added lateral MIC of silicon [76]. **b** In₂O₃ NWs grown at 550°C at 2,300 V/cm [77]

Fig. 10 AFM images for
a electric field nanostructured
50-nm-thin nickel film for
2 kV/cm for electric field
parallel to the substrate plane,
b electric field nanostructured
nickel thin film for 0.16 kV/cm
for electric field normal to the
substrate plane, **c** electric field
nanostructured 100-nm-thin
nickel film for 1.2 kV/cm for
electric field parallel to the
substrate plane, **d** electric field
nanostructured 30-nm-thin
indium film for 2.66 kV/cm for
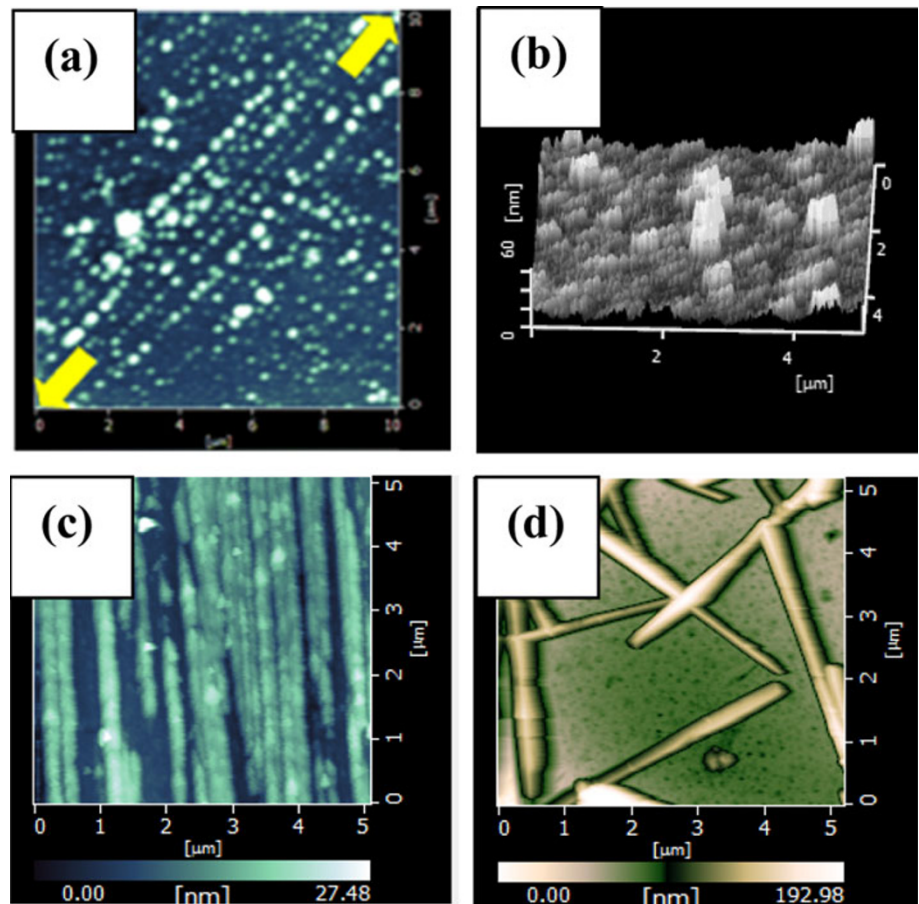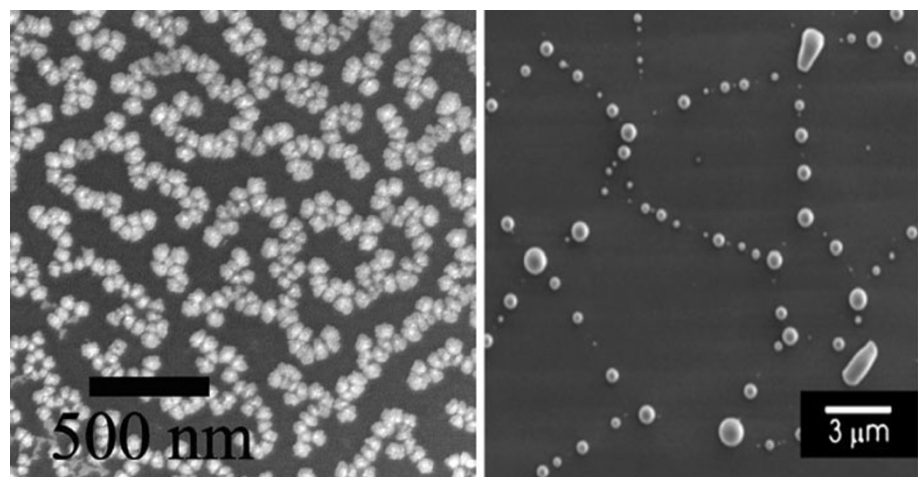electric field parallel to the
substrate plane [79, 81]

Fig. 11 **a** Excimer laser
nanostructured silicon wafer
nanoparticles formed at
0.6 J/cm^2, 450 pulses, 100 Torr
He [85]. **a** 15-nm Ni films [86],
**b** excimer laser nanostructured

deposits back on the surface due to back air pressure in aligned manner (as shown in Fig. 9b).

Electric field–induced nanostructuring effects, such as organization into an array of nanoparticles, formation of nanowires and transition from amorphous to nanocrystal-line states, has been demonstrated for thin film surfaces. Grain growth, crystalline growth and the alignment—these three have three distinct field thresholds. It is further shown

that the nanostructures can be manipulated by simply changing the direction of the applied field. High fields cause field-induced emission in the films. It is observed that while the microstructural reconstruction of the surfaces can be manipulated, the amorphous–crystalline transition is irreversible [79]. Electric field–induced effects are having such substantial effects on grain size that it can work as a tool to play with the surface plasmonic modes of gold and

Fig. 12 AFM images at a laser fluence of 5 J/cm^2 for 8 shots at **a** 10° angles of incidence, **b** 20° angles of incidence, **c** atomic force microscope image. AFM images for silicon surface irradiated at laser fluence of 0.15 J/cm^2 and 90° angle of incidence in the proximity of **c** 25-micron-thick blade edge mask and **c** 30 micron diameter copper wire mask [87]
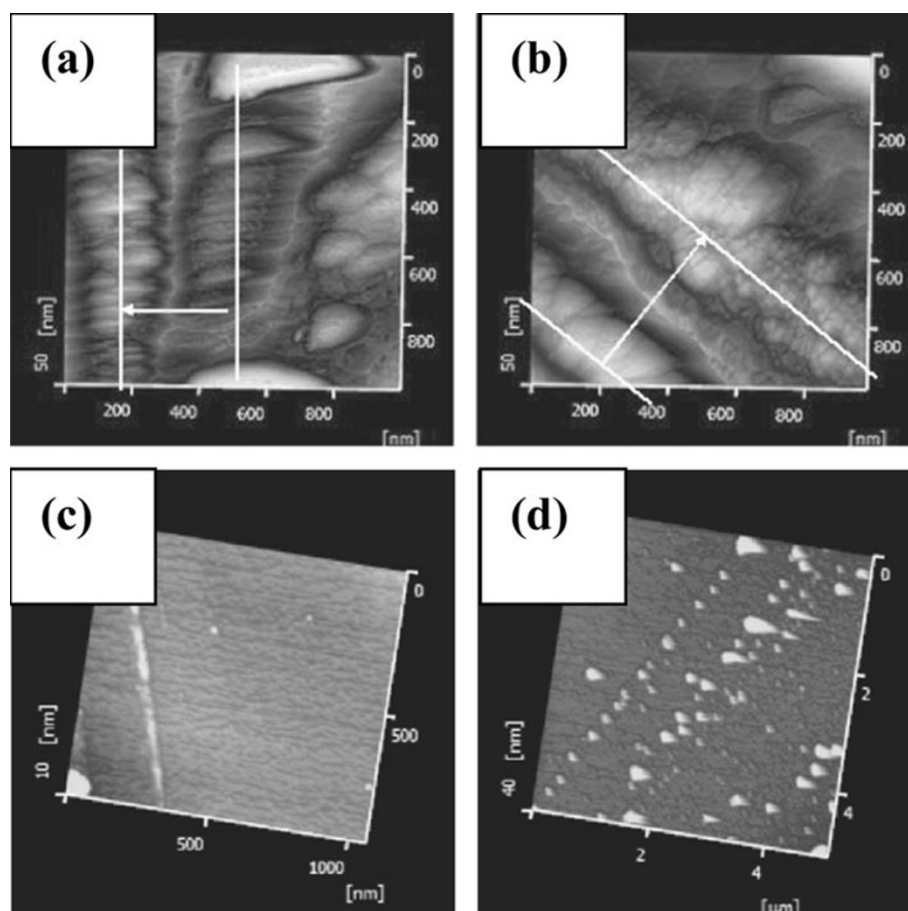
indium [80]. For 50-nm-thin nickel film, electric field application has given rise to the growth of array of nickel nanodots (as shown in Fig. 10a). When 100-nm nickel thin film was undergone through 0.66 kV/cm electric field, nanowires do grow on the surface [81] (as shown in Fig. 9c). Indium metal however having low melting point has shown less critical field for nanowire growth compared to nickel metal (as shown in Fig. 10d). Application of vertical electric field can give rise to vertical nanopillars [79, 82] (as shown in Fig. 10b). Electric field–mediated nickel-induced nanocrystallization of amorphous silicon thin films in the complete absence of external heating has also been reported [83]. Electric field–induced nanostructuring has been a potential technique for nanotechnology-driven applications [64, 84].

Laser-Induced Self-Assembly

Laser has earlier been reported to be used for self-assembly for silicon surface [85] (as shown in Fig. 11a) and metallic thin film of nickel [86] (as shown in Fig. 11b).

Current author has irradiated KrF excimer laser onto silicon surface [87] at very small angles to achieve linearly self-assembled features (as shown in Fig. 11a, b). At 20° angle of incidence, in-plane growth of nanowires (Fig. 11b) consisted of fine nanoparticles (15–30 nm) was observed. One another technique was developed by the current author to utilize elevated temperature near micron-sized mask edge to achieve growth of silicon nanowires. Mask height and radius of curvature decide the kind of growth features when laser-evaporated silicon material redeposit on the silicon surface. Copper wire and stainless steel blades were made use of for this purpose (Fig. 12).

Future Scope

Directed self-assembly has been proven to be quite handy for chemists, physicists and biologists alike and more importantly to materials scientists. Various kinds of materials starting from elemental materials to oxides, nitrides, superconductors, magnetic materials, dielectrics have been self-assembled using some template or field as a guide. Cracks, nanopores, V-grooves and various other surface patterns have already been used as physical templates. One such example is the use of carbon nanotube as template for further vapour growth [88]. It has to be kept in

mind that lithography itself can conveniently be used to direct the growth. Unsatisfied bonds have been conveniently used as chemical templates. Similarly, biologists too have employed bio-alignments (DNA as template is one example). Electric field, excimer laser, light, magnetic field, pressure gradient, shear gradient and various fields have been employed to achieve functional nanostructures by field-directed self-assembly. Here in this review, use of electric field and laser has been described in detail. However, magnetic field [89, 90] and focused ion beam [91] are the other two fields as competitive for the purpose of directed self-assembly of materials. Directed self-assembly of nanomaterials as a discipline is quite versatile in nature. Guise et al. [92] has achieved patterning of sub-10-nm Ge islands on Si(100) by directed self-assembly. Greve et al. [93] have dealt with the directed self-assembly of amphiphilic regioregular polythiophenes on the nanometer scale.

Xu et al. [94] have demonstrated directed self-assembly of block copolymers on two-dimensional chemical patterns fabricated by electro-oxidation nanolithography. Gupta et al. [95] have described the entropy-driven segregation of nanoparticles to cracks in multilayered composite polymer structures. Adam et al. [96] have used NH···O hydrogen bonding for directed self-assembly and achieved a trilayered supramolecular array formed between 1,2-diaminoethane and benzoic acid. Lee et al. [97] have achieved self-assembly of 2,6-dimethylpyridine on Cu(1 1 0) directed by weak hydrogen bonding. Kinge et al. [98] have reviewed self-assembling of nanoparticles at surfaces and interfaces. Sitti [99] has demonstrated high aspect ratio polymer micro/nanostructure manufacturing using directed self-assembly.

Even though science and technology of directed self-assembly has advanced manifold, this part of nanotechnology as a pursuit of research and development is still young. To industrialize this technique, control of material growth has to be understood at atomic scale. Accurate prediction and tailoring of physical properties at nanoscale are still a challenge.

References

1. S.H.M. Jafri, A.B. Sharma, C. Thanachayanont, J. Dutta, Mater. Res. Soc. Symp. Proc. **901E**, 0901-Rb18-01.1 (2006)
2. J.F. Conley Jr, L. Stecker, Y. Ono, Nanotechnology **16**, 292 (2005)
3. X. Xiong, C.L. Chen, P. Ryan, A.A. Busnaina, Y.J. Jung, M.R. Dokmeci, Nanotechnology **20**, 295302 (2009)
4. J.Y. Cheng, C.T. Rettner, D.P. Sanders, H.C. Kim, W.D. Hinsberg, Adv. Mater. **20**, 3155 (2008)
5. J.Y. Cheng, J. Pitera, O.H. Park, M. Flickner, R. Ruiz, C.T. Black, H.C. Kim, Appl. Phys. Lett. **91**, 143106-1 (2007)
6. J.A. Liddle, Y. Cui, P. Alivisatos, Lithographically directed self-assembly of nanostructures. J. Vac. Sci. Technol. B **22**, 3409 (2004)
7. A. Winkleman, B.D. Gates, L.S. McCarty, G.M. Whitesides, Adv. Mater. **17**, 1507 (2005)
8. M. Lu, M.W. Jang, G. Haugstad, S.A. Campbell, T. Cui, Appl. Phys. Lett. **94**, 261903-1 (2009)
9. T. Vossmeyer, E.D. Ionno, J.R. Heath, Angew. Chem. Int. Ed. Engl. **36**, 1080 (1997)
10. J. Sun, M. Gao, J. Feldmann, J. Nanosci. Nanotechnol. **1**, 133 (2001)
11. R.D. Deegan, Phys. Rev. E **61**, 475 (2000)
12. R.D. Deegan, O. Bakajin, T.F. Dupont, G. Huber, S.R. Nagel, T.A. Witten, Nature **389**, 827 (1997)
13. R.D. Deegan, O. Bakajin, T.F. Dupont, G. Huber, S.R. Nagel, T.A. Witten, Phys. Rev. E **62**, 756 (2000)
14. E. Adachi, A.S. Dimitro, K. Nagayama, Langmuir **11**, 1057 (1995)
15. H. Hu, R.G. Larson, J. Phys. Chem. B **106**, 1334 (2002)
16. E. Rabani, D.R. Reichman, P.L. Geissler, L.E. Brus, Nature **426**, 271 (2003)
17. T.P. Bigioni, X.-M. Lin, T.T. Nguyen, E.I. Corwin, T.A. Witten, H.M. Jaeger, Nat. Mater. **5**, 265 (2006)
18. R.V. Hameren, P. Schon, A.M. Buul, J.S. Hoogboom, V. Lazarenko, J.W. Gerritsen, J.A.A.W. Elemans, R.J.M. Nolte, Science **314**, 1433 (2006)
19. J.X. Huang, F. Kim, A.R. Tao, Nat. Mater. **4**, 896 (2005)
20. C.P. Martin, M.O. Blunt, E. Pauliac-Vaujour, A. Stannard, P. Moriarty, I. Vancea, U. Thiele, Phys. Rev. Lett. **99**, 116103 (2007)
21. P. Moriarty, M.D.R. Taylor, M. Brust, Phys. Rev. Lett. **89**, 248303 (2002)
22. L. Shmuylovich, A.Q. Shen, H.A. Stone, Langmuir **18**, 3441 (2002)
23. Z.Q. Lin, S. Granick, J. Am. Chem. Soc. **127**, 2816 (2005)
24. S.W. Hong, J. Xu, J. Xia, Z. Lin, F. Qiu, Y. Yang, Chem. Mater. **17**, 6223 (2005)
25. J. Xu, J. Xia, S.W. Hong, Z.Q. Lin, F. Qiu, Y.L. Yang, Phys. Rev. Lett. **96**, 066104 (2006)
26. J. Xu, J. Xia, S.W. Hong, Z.Q. Lin, Angew. Chem. Int. Ed. **46**, 1860 (2007)
27. M. Byun, S.W. Hong, L. Zhu, Z.Q. Lin, Langmuir **24**, 3525 (2008)
28. M. Byun, S.W. Hong, F. Qiu, Q. Zou, Z. Lin, Macromolecules **41**, 9312 (2008)
29. M. Byun, R. Laskowski, M. He, F. Qiu, M. Jeffries-El, Z. Lin, Soft Matter **5**, 1583 (2009)
30. S.W. Hong, M. Byun, Z. Lin, Angew. Chem. Int. Ed. **48**, 512 (2009)
31. S.W. Hong, J. Wang, Z.Q. Lin, Angew. Chem. Int. Ed. **48**, 8356 (2009)

32. C.A. Neugebauer, Condensation, nucleation and growth of thin films, in *Handbook of Thin Film Technology, Chap. 8*, ed. by L.I. Maissel, R. Glang (McGraw Hill, New York, 1970), p. 8.3
33. J.P. Spatz, S. Mössmer, C. Hartmann, M. Möller, T. Herzog, M. Krieger, H.G. Boyen, P. Ziemann, B. Kabius, Langmuir **16**, 407 (2000)
34. W.A. Lopes, H.M. Jaeger, Nature **414**, 735 (2001)
35. R.A. Pai, R. Humayun, M.T. Schulberg, A. Sengupta, J.-N. Sun, J.J. Watkins, Science **303**, 507 (2004)
36. M. Templin, A. Franck, A.D. Chesne, H. Leist, Y. Zhang, Science **278**, 1795 (1997)
37. H.J. Liang, T.E. Angelini, J. Ho, P.V. Braun, G.C.L. Wong, J. Am. Chem. Soc. **125**, 11786 (2003)
38. M. Li, H. Schnablegger, S. Mann, Nature **402**, 393 (1999)
39. M.R. Bockstaller, Y. Lapetnikov, S. Margel, E.L. Thomas, J. Am. Chem. Soc. **125**, 5276 (2003)
40. W. Shenton, D. Pum, U.B. Sleytr, S. Mann, Nature **389**, 585 (1997)
41. S. Mann, G.A. Ozin, Nature **382**, 313 (1996)
42. T.T. Albrecht, J. Schotter, G.A. Kästle, N. Emley, T. Shibauchi, Science **290**, 2126 (2000)
43. M. Bockstaller, R. Kolb, E.L. Thomas, Adv. Mater. **13**, 1783 (2001)
44. C.T. Black, C.B. Murray, R.L. Sandstrom, S.H. Sun, Science **290**, 1131 (2000)
45. C. Sanchez, B. Lebeau, MRS Bull. **26**, 377 (2001)
46. M. Alexandre, P. Dubois, Mater. Sci. Eng. Rev. **28**, 1 (2000)
47. P. Soo, B. Huang, Y.I. Jang, Y.M. Chiang, D.R. Sadoway, A.M. Mayes, J. Electrochem. Soc. **146**, 32 (1999)
48. A.C. Balazs, Curr. Opin. Colloid Interface Sci. **4**, 443 (2000)
49. J.Y. Lee, Z. Shou, A.C. Balazs, Phys. Rev. Lett. **91**, 136103 (2003)
50. J.Y. Lee, Z. Shou, A.C. Balazs, Macromolecules **36**, 7730 (2003)
51. Y. Lin, A.B. Ker, J. He, K. Sill, H. Xiang, C. Abetz, X. Li, J. Wang, T. Emrick, S. Long, Q. Wang, A. Balazs, T.P. Russell, Nature **434**, 55 (2005)
52. S.W. Hong, W. Jeong, H. Ko, M.R. Kessler, V.V. Tsukruk, Z. Lin, Adv. Funct. Mater. **18**, 2114 (2008)
53. S. Wang, G.J. Yu, J.L. Gong, D.Z. Zhu, H.H. Xia, Nanotechnology **18**, 015303 (2007)
54. Q. Guo, X. Mei, H. Ruda, T. Tanaka, M. Nishio, H. Ogawa, Jpn. J. Appl. Phys. **42**, L508 (2003)
55. S.K. Park, J.S. Noh, W.B. Chin, D.D. Sung, Curr. Appl. Phys. **7**, 180 (2007)
56. M.T. Wu, I.C. Leu, J.H. Yen, M.H. Hon, Solid State Lett. **7**, C61 (2004)
57. F. Zheng, L. Liang, Y. Gao, J.H. Sukamto, C.L. Aardahl, Nano Lett. **2**, 729 (2002)
58. W.H. Kim, S.J. Park, J.Y. Son, H. Kim, Nanotechnology **19**, 045302 (2008)
59. S. Shingubara, J. Nanopart. Res. **5**, 17 (2003)
60. N. Ravishankar, V.B. Shenoy, C.B. Carter, Adv. Mater. **16**, 76 (2004)
61. E.J. Boyd, S.A. Brown, Nanotechnology **20**, 425201 (2009)
62. P. Kumar, M.G. Krishna, A.K. Bhatnagar, A.K. Bhattacharya, Int. J. Nanomanuf. **2**, 477 (2008)
63. P. Kumar, J. Nanopart. Res. doi:10.1007/s11051-009-9813-9
64. M.G. Krishna, P. Kumar, Non-lithographic techniques for nanostructuring thin films and surfaces, in *Emerging nanotechnology for manufacturing*, ed. by W. Ahmed, M.J. Jackson (Elsevier, The Netherlands, 2009)
65. S. Asaf, A.S. Ella, B. Uri, J. Am. Chem. Soc. **128**, 10006 (2006)
66. M. Fujita, Chem. Soc. Rev. **27**, 417 (1998)
67. R.A. Mcmillan, C.D. Paavola, J. Howard, S.L. Chan, N.J. Zaluzec, J.D. Trent, Nat. Mater. **1**, 247 (2002)
68. T.A. Taton, C.A. Mirkin, R.L. Letsinger, Science **289**, 1757 (2000)
69. J.W. Liu, Y. Lu, J. Am. Chem. Soc. **125**, 6642 (2003)
70. J.W. Liu, Y. Lu, Angew. Chem. Int. Ed. **45**, 90 (2006)
71. K. Keren, R.S. Berman, E. Buchstab, U. Sivan, E. Braun, Science **302**, 1380 (2003)
72. H. Yao, C. Yi, C.H. Tzang, J. Zhu, M. Yang, Nanotechnology **18**, 015102 (2007)
73. R. Pasquino, F. Snijkers, N. Grizzuti, J. Vermant, Langmuir **26**, 3016 (2010)
74. L.S. McCarty, A. Winkleman, G.M. Whitesides, Angew. Chem. **119**, 210 (2006)
75. R. Basu, G.S. Iannacchione, arXiv:0812.1585v1 [cond-mat.soft]
76. Y. Wang, L. Wang, B. Tang, D.K. Choi, Thin Solid Films **515**, 2507 (2006)
77. S.Q. Li, Y.X. Liang, T.L. Guo, Z.X. Lin, T.H. Wang, Mater. Lett. **60**, 1492 (2006)
78. P. Kumar, Micro. Nano. Lett. **5**, 110 (2010)
79. P. Kumar, M.G. Krishna, A.K. Bhattacharya, Int. J. Nanosci. **7**, 255 (2008)
80. P. Kumar, M.G. Krishna, Phys. Stat. Sol. (a) **207**, 947 (2009)
81. P. Kumar, Adv. Sci. Lett. **3**, 62 (2010)
82. P. Kumar, Nano. Trends **6**(3), (2009)
83. P. Kumar, Appl. Phys. A **98**, 473 (2010)
84. P. Kumar, in *Employing Electrical Energy in Nanotechnology*, ed. by H.S. Nalwa, in a edited book series "Encyclopedia of nanoscience and nanotechnology" (American Scientific Publishers, 2010), ISBN: 1-58883-159-0
85. A.J. Pedraza, J.D. Fowlkes, Y.F. Guan, Appl. Phys. A **77**, 277 (2003)
86. S.J. Henley, J.D. Carey, S.R.P. Silva, Appl. Surf. Sci. **253**, 8080 (2007)
87. P. Kumar, M.G. Krishna, A.K. Bhattacharya, J. Nanosci. Nanotechnol. **9**, 3224 (2009)
88. W.K. Wong, S.H. Lim, J.T.L. Thong, Nanotechnology **17**, 2373 (2006)
89. Y. Sahoo, M. Cheon, S. Wang, H. Luo, E.P. Furlani, P.N. Prasad, J. Phys. Chem. B **108**, 3380 (2004)
90. H. Niu, Q. Chen, H. Zhu, Y. Lin, X. Zhang, J. Mater. Chem. **13**, 1803 (2003)
91. Y. Du, S. Atha, R. Hull, J.F. Groves, I. Lyubinetsky, D.R. Baer, Appl. Phys. Lett. **84**, 5213 (2004)
92. O. Guise, J. Ahner, J. John, T. Yates, V. Vaithyanathan, D.G. Schlom, J. Levy, Appl. Phys. Lett. **87**, 1902 (2005)
93. D.R. Greve, N. Reitzel, T. Hassenkam, J. Bøgelund, K. Kjaer, P.B. Howes, N.B. Larsen, M. Jayaraman, R.D. McCullough, T. Bjørnholm, Synth. Met. **102**, 1502 (1999)
94. J. Xu, S. Park, S. Wang, T.P. Russell, B.M. Ocko, A. Checco, Adv. Mater. doi:10.1002/adma.200903640
95. S. Gupta, Q. Zhang, T. Emrick, A.C. Balazs, T.P. Russell, Nat. Mater. **5**, 229 (2006)
96. K.R. Adam, I.M. Atkinson, R.L. Davis, L.F. Lindoy, M.S. Mahinay, B.J. McCool, B.W. Skelton, A.H. White, Chem. Commun. **467**, 5/05748I (1997)
97. J. Lee, D.B. Dougherty, J.T. Yates Jr, Surf. Sci. **601**, L91 (2007)
98. S. Kinge, M.C. Calama, D.N. Reinhoudt, Chem. Phys. Chem. **9**, 20 (2007)
99. M. Sitti, in *Proceedings of the 2003 IEEEHASME Intl. Conf. Adv. Intelligent Mechatronics (AIM 2003) IEEE 886*, 0-7803-7759-1/03 (2003)